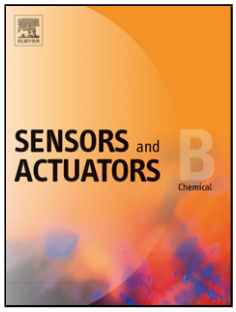

Title: High-performance optical fiber humidity sensor based on lossy mode resonance using a nanostructured polyethylenimine and graphene oxide coating

Authors: Miguel Hernaez, Beatriz Acevedo, Andrew G. Mayes, Sonia Melendi-Espina

PII: S0925-4005(19)30179-0
DOI: https://doi.org/10.1016/j.snb.2019.01.145
Reference: SNB 26071

To appear in: *Sensors and Actuators B*

Received date: 30 July 2018
Revised date: 15 January 2019
Accepted date: 28 January 2019

Please cite this article as: Hernaez M, Acevedo B, Mayes AG, Melendi-Espina S, High-performance optical fiber humidity sensor based on lossy mode resonance using a nanostructured polyethylenimine and graphene oxide coating, *Sensors and amp; Actuators: B. Chemical* (2019), https://doi.org/10.1016/j.snb.2019.01.145

High-performance optical fiber humidity sensor based on lossy mode resonance using a nanostructured polyethylenimine and graphene oxide coating

[a]Miguel Hernaez[*], [b]Beatriz Acevedo, [a]Andrew G. Mayes and [b]Sonia Melendi-Espina[*]

[a]School of Chemistry, Faculty of Science, University of East Anglia, Norwich Research Park, Norwich, NR4 7TJ, UK

[b]Engineering, Faculty of Science, University of East Anglia, Norwich Research Park, Norwich, NR4 7TJ, UK

[*]Correspondence: m.hernaez@uea.ac.uk, s.melendi-espina@uea.ac.uk

Tel.: +44 (0) 1603592848

HIGHLIGHTS:

- Layer-by-layer assembly has been proven as an effective thin film deposition method
- Good coverage, continuity and controlled thickness of the sensitive film accomplished
- The fabricated sensor exhibits very good sensitivity and a wide detection range
- Hysteresis as well as response and recovery times are excellent

ABSTRACT:

In this study, a rapid optical fiber sensor for humidity with high sensitivity and wide detection range has been constructed, based on lossy mode resonance (LMR). A thin film made of alternating polyethylenimine (PEI) and graphene oxide (GO) layers was selected as sensitive coating. It was deposited on a SnO_2-sputtered fiber core in a dip-assisted layer-by-layer assembly. The structure and surface chemistry of the raw materials were investigated by means of Fourier transform infrared spectroscopy and X-ray photoelectron spectroscopy. Key properties such as sensitivity, linearity, hysteresis, stability and response and recovery times were characterized. The sensor exhibited excellent sensitivity, especially at high relative humidity (RH) levels, and short reaction and retrieval periods. This research provides a viable and practical way to fabricate high performance humidity optical fiber sensors with GO-based nanostructured coatings.

KEYWORDS:

Optical fiber sensor, relative humidity sensor, breathing monitoring, lossy mode resonance, graphene oxide, layer-by-layer

1. INTRODUCTION

Humidity measurement and control are essential in many industrial and agricultural processes as well as human activities, such as air quality monitoring, air conditioning, manufacturing processes, control and storage of food or computer components [1-4]. High sensitivity, wide humidity detection range, rapid response and short recovery times are the key features that humidity sensors must achieve in order to fulfil our needs. A key factor that determines the humidity sensor's behavior is the selected sensing material. Polymers have previously been employed as humidity sensitive materials [5-8] due to their cost-effectiveness, relatively simple production, compactness and excellent performance. However, polymers still exhibit limitations, such as hysteresis of the response, limited sensing range, drifting, and poor durability against water or dew, which damage sensors' functionality [6, 9, 10]. For example Polyethylenimine (PEI) is a polymer that has been widely used as a humidity sensitive coating [6, 10]. However, these PEI-based sensors cannot measure relative humidity (RH) when it exceeds 80 % [10].

Numerous methods have been attempted to improve polymeric performance of polymer-coated sensors, such as cross-linking of polymers chains, quaternization, and copolymerization with hydrophobic monomers [6, 11, 12]. Recent studies have demonstrated that the humidity-sensing properties of pure polymers could be improved by introducing an additional material, i.e. by making composites [13-15]. In this regard, graphene oxide has attracted much attention as a potential candidate to improve polymeric sensor response characteristics [9, 14, 16].

Graphene oxide (GO) is a non-stoichiometric material with a graphene-like structure. It consists of aromatic carbon randomly interspersed with oxygen containing functional groups (epoxy, carboxyl and hydroxyl functionalities). Significant qualities like hydrophilicity and high dispersion in various solvents, due to the presence of oxygenated functional groups, makes GO a suitable material for sensing applications [17, 18]. Therefore, the development of composites including GO offers a new way forward for fabrication of high performance humidity-sensitive coatings.

Several types of humidity sensors have been developed over the years [19]. Optical fiber sensors have attracted increasing attention due to their benefits over traditional sensors, such as small size, biocompatibility, remote sensing capability and safety in flammable environments [20, 21]. Across the range of optical fiber sensors available, those based on electromagnetic resonances are very popular as they are reliable, robust and very sensitive [22, 23]. When an optical fiber is coated with a thin-film, different cases of electromagnetic resonances can be generated depending on the properties of the materials involved in the system (the waveguide, the coating and the external medium). These resonances produce a

stable absorption band in the transmitted spectrum that shifts in wavelength if there is a variation in the refractive index of the coating or the surrounding medium. Then, if the refractive index of the coating is sensitive to a desired target, the variation of this target will lead to a shift in the absorption peak. This shift can be measured and is the basis of the sensing mechanism [22, 23].

Sensors based on lossy mode resonance (LMR) constitute a particularly promising research field since they are independent of the polarization of light and enlarge the range of materials available for sensor surface coating, from noble metals to metal oxides, polymers and many others [23].

Consequently, to fabricate an optical fiber sensor based on LMR it is therefore essential to deposit a good quality and uniform thin-film with controlled thickness onto the fiber core. Several fabrication techniques have been deployed in the preparation of thin films for different applications. However, layer-by-layer (LbL) assembly has been considered by the scientific community as a very promising and cost-effective method that shows significant advantages in comparison with other thin-film deposition techniques, such as low cost, simplicity in operation and coating uniformity [24-26]. Furthermore, LbL assembly has been selected in this study because it allows the monitoring of the shift of the LMR bands while depositing the sensitive coating.

LbL assembly involves the sequential deposition of two different substances, which are interconnected either by chemical reactions (covalent bonding) or electromagnetic attraction [27]. PEI does possess high amine density and accessible primary amine sites on the end of the chains [28], which in turn have great affinity to the oxygen functional groups on the basal plane and edges of GO [28]. Therefore, PEI and GO are ideal candidates for the fabrication of composite materials by means of LbL.

Consequently, the aim of this study was to fabricate a rapidly-responding humidity sensor with high sensitivity and wide detection range. To reach this goal, an LMR optical fiber sensor based on a sputtered SnO_2 coating was fabricated and characterized. It was then modified by depositing multilayer coatings including PEI and GO onto the SnO_2 layer by means of dip-assisted layer-by-layer deposition. The device was characterized in terms of sensitivity, linearity, hysteresis and response times. To the extent of the authors' knowledge, this study presents the first optical fiber humidity sensor based on the LMR phenomena that includes GO in the sensitive coating.

2. MATERIALS AND METHODS

The experimental aspects of this research, such as the fabrication of the sensing devices, the characterization setup and procedure are explained in this section.

2.1. Materials and sensor fabrication

The LMR-based optical fiber sensing scheme consisted of a multimode optical fiber with a layer of SnO_2 directly sputtered onto the core, which performs as LMR-supporting coating [29] and a graphene-based thin film deposited on top, acting as sensitive coating. Therefore, in order to fabricate the sensor, the cladding of a 200 µm-core multimode optical fiber (FT200EMT, purchased from Thorlabs, Inc.) was thermally removed. Subsequently, the core

was sonicated and cleaned in detergent and acetone and rinsed with ultrapure water. Following the cleaning process, the SnO_2 film was sputtered (K675XD sputter coater from Quantum Technologies) for 150 seconds, during which the substrate was subjected to a continuous rotation to ensure the uniformity of the film. This SnO_2 layer will generate the LMR absorption bands.

A 2 cm fragment of the coated fiber was perpendicularly cleaved (NorthLab ProCleave LD II cleaver) and spliced (Fitel S178A fusion splicer) to 200 µm optical fiber core pigtails; and connected to the characterization setup (Figure 1) to follow the generation and the shift of the LMR absorption peak during the construction of the sensitive coating.

The sensitive layer was deposited by dip-assisted layer-by-layer coating, as it is an effective method for fabricating good quality thin films [30, 31]. In a layer-by-layer assembly the film layer is adhered to the substrate and interconnected interchangeably with another substance either by chemical reactions (covalent bonding) or electromagnetic attraction [27].

Poly(ethyleneimine) (PEI) solution in deionized water (DI) from Sigma Aldrich (CAS Number 9002-98-6) and GO powder from Graphenea S.A. were selected for the layer-by-layer assembly. Five bilayers were deposited onto the SnO_2-coated optical fiber fragment. PEI solution (2 mg ml^{-1}) and GO suspension (0.5 mg ml^{-1} in water) were stirred overnight and the GO was also sonicated for 30 minutes before deposition. The sputtered fiber was submerged into a 1M KOH solution for 30 minutes and then rinsed thoroughly with DI water. Then, the substrate was immersed into the PEI solution for 5 minutes. Following this step, the substrate was washed with DI water to remove surplus material and dried in air. The substrate was then immersed in the GO dispersion for 5 minutes, before being rinsed with DI water and dried. The final coating was obtained by repeating these steps 5 times.

It is known that the charge density of the materials involved affects the adsorption efficiency onto the self-assembled thin film, while the ionization degree is greatly affected by the pH of the solutions [27, 32]. pH of the GO suspension was adjusted to 5.2 and 8.3 for PEI using HCl or NaOH diluted in water. These values were suggested in the literature as the optimum values to perform a successful layer-by-layer deposition and ensure good adsorption efficiency between both materials [32]. The refractive index of the PEI/GO coating is highly sensitive to RH variations. Consequently, a RH alteration leads to a shift in wavelength of the LMR band generated by the SnO_2 layer. This shift can be measured and this is the basis of the sensing mechanism.

2.2. Coating characterization

X-ray photoelectron spectroscopy (Thermo Scientific K-Alpha X-ray Photoelectron Spectrometer (XPS) System) was used to characterize the surface chemistry of GO. FT-IR absorption spectra of PEI and GO were recorded on a Nicolet stepscan FTIR spectrometer with diamond ATR.

An FEI NanoSEM 450 FEG scanning electron microscope (SEM) was used to acquire an image of the cross section of the fiber coated with the sputtered film of SnO_2.

Film uniformity and texture were also characterized by means of the scanning electron microscope. Its thickness was estimated by means of a DektakXT Stylus Profiler (Bruker). Ten

measurements were taken per sample in two different specimens. The final thickness was calculated as the average of all these values.

2.3. Sensor characterization

Figure 1 shows the transmission setup used to characterize the sensor. A halogen white light source (HL2000, Oceanoptics Inc.) was connected to one of the optical fiber pigtails to couple light into the sensing device. The coupled light passed through the sensor, reached a spectrometer (Oceanoptics USB2000) connected to the other pigtail, and the spectra of the transmitted light through the sensor were collected. In this way, it was possible to monitor the generation and the shift of the LMR absorption peak during the construction of the PEI/GO coating onto the fiber core.

To characterize the static and dynamic responses of the device as a humidity sensor, it was introduced in a Binder KMF 115 environmental chamber, varying the relative humidity (RH) from 20 %-90 %, and collecting the transmitted spectra. A MatLab routine was created to consistently obtain the wavelengths at which the LMR bands are centered. It returns the coefficients for a polynomial of degree 2 that is the best fit for each LMR peak. The wavelength at which the maximum of the curve is located is then numerically calculated.

Humidity was regulated using a capacitive humidity sensor and steam humidification. All the measurements were performed at constant temperature (20 °C).

In addition, the sensor was dynamically characterized as a breathing sensor.

3. RESULTS

In this section, the characterization of the materials and sensitive coating, the monitoring of the coating deposition and the behavior of the device as relative humidity sensor as well as breathing sensor are presented.

3.1. Characterization of the LMR supporting coating and the sensitive coating

GO spectrum exhibits several peaks related to the oxygen functional groups, which confer its hydrophilicity (Figure 2). The band at around 3400 cm^{-1} and the sharp peak at 1630 cm^{-1}, correspond to the stretching and bending vibration of OH groups, respectively [33-35]. The absorption peak at 1720 cm^{-1} arises from C=O stretching vibration of carboxyl groups, while bands located at 1395 cm^{-1}, 1340 cm^{-1} and 1060 cm^{-1} are assigned to vibration of O-H, C-OH and C-O groups [33-35]. The band at 1270 cm^{-1} corresponds to the stretching vibration of C-O in the epoxy groups [33-35].

The PEI spectrum presents the characteristic peak at 1650 cm^{-1}, which arises from bending of the amine (-N-H) group present in this polymer [36]. The N-H stretching bands at around 3300 cm^{-1} are also prominent [36].

To study in detail the surface chemistry of the selected GO, wide-scan spectra in the binding energy range of approximately 0–1000 eV was obtained by means of XPS in order to identify the elements present on its surface and to perform a quantitative analysis. Carbon and oxygen have been mainly detected in the wide scan spectra, with a C/O ratio of 2.1 (Table 1).

Careful curve fitting was performed on the C(1s) spectrum to quantitatively differentiate the five carbon stages: sp^2-hybridised carbon atoms (284.4 eV), sp3-hybridised carbon atoms

(285.5-285.7 eV), the C–O of alcohol/epoxy groups (286.3-286.8), the C=O of carbonyl groups (287.6-287.7 eV), and C(O)OH of carboxylic acid (288.5-289.0 eV) [37]. The π–π* shake-up signal (290.7-291.3 eV) is also present, which is typical for sp^2-hybridized carbon [37] (Table 1).

C(1s) XPS spectra of GO indicates a considerable degree of oxidation, exhibiting different oxygen functional groups in GO surface (e.g. carbonyl, epoxy, hydroxyl groups) [38]. GO contains carboxyl and hydroxyl groups on the edges of its basal plane, lending it its hydrophilic character [35].

With both materials (GO and PEI), a coating consisting of five bilayers of PEI/GO has been deposited onto a SnO_2-coated structure to obtain a device sensitive to external relative humidity changes. The high COOH content of the GO confers a negative charge, which provides strong interaction with the positive charge of the amine groups in the PEI, thus generating a strongly-bonded and stable layer by layer structure.

The SnO_2 layer sputtered onto the fiber core (LMR supporting coating) seems to be very homogeneous and uniform (Figure 3), showing an average thickness of 220 nm. The thickness was measured in five different areas of the optical fiber.

Essential to developing efficient sensitive coatings is the ability to fabricate uniform films and control their thickness. Among the broad range of available deposition techniques, dip-assisted layer-by-layer is an effective method of fabricating good quality thin films. Low cost, simplicity in operation and coating uniformity are key advantages of this method.

To properly study the homogeneity, uniformity and thickness of the sensitive coating placed onto the SnO_2-coated optical fiber core, it was also deposited onto a planar silicon-based substrate. Figure 4 shows a very good coverage and continuity of the sensitive film, confirming the accomplishment of the dip-assisted layer-by-layer assembly as suitable deposition technique.

The thickness of the fabricated film was analyzed by means of a DektaKXT profiling system. As previously mentioned, thickness was estimated as the average of 10 measurements taken in two different samples. The results are very consistent and repeatable, showing a thickness of 23.3 nm and a standard deviation of 2.6 nm.

3.2. Construction of the sensors

The first step was to monitor the generation and shift of the LMR peak. As soon as the SnO_2-coated fiber (0 bilayers) is connected to the transmission setup shown in Figure 1, part of the optical power is transmitted through the coating and lost, generating an LMR [23]. Accordingly, an absorption peak is produced, and it can be perceived in the transmitted spectrum, being in this case centered at 420 nm when the device is in air (Figure 5).

The resonance wavelength of these devices shifts to higher wavelengths when the external medium refractive index is increased [23, 39], which occurs when bilayers of PEI/GO are deposited onto it. The LMR peak in air then moves from 439 nm when one PEI/GO bilayer is deposited onto the SnO_2-sputtered fiber to 536 nm after the deposition of 5 bilayers, as shown in Figure 5.

The deposition process was stopped after 5 bilayers, as previous results show this thickness is a good compromise between sensitivity and sensor response [31]. In addition, it is known that the LMR absorption peak will shift to the right when the external relative humidity increases [40], therefore the device can be characterized as a humidity sensor within the wavelength range of the available spectrometer.

3.3. Static response to relative humidity

The static response of the fabricated sensor as a humidity sensing device was characterized by introducing it into a Binder KMF 115 environmental chamber at 20 °C. The relative humidity varied from 20 %-90 % with increasing 10 % RH steps and ensuring that enough time is given for measurements to stabilize.

The device shows a shift of the resonance peak to higher wavelengths with increasing relative humidity (Figure 6). This is due to the interaction of water with the GO and PEI elements of the coating, which causes a variation of the coating refractive index [40].

The hysteresis of the fabricated sensor was also investigated, studying its response with increasing and decreasing RH, accomplishing an average hysteresis value of 1.1 %. Consequently, there is a very good agreement between both evolutions, as shown in Figure 6, which demonstrates that this sensor has excellent reversibility under RH variations.

The average sensitivity across the complete range of study (20 %RH – 90 %RH) achieves 0.612 nm/%RH (estimated in the increasing RH graph) and 0.600 nm/%RH in the decreasing RH curve).

However, as shown in Figure 6, the sensitivity of the sensor is not constant over the whole interval of RH. Sensitivity varies depending on the RH, which has been previously reported in prior studies carried out using different sensitive coatings [40].

The response of our sensor can be adequately described by two linear intervals. The first stage covers RH ranging from 20 % to 70 % and the second interval from 70 % to 90 %. In the first range, the sensitivity is linearly fitted to be 0.317 nm/%RH (estimated in the increasing RH curve) and 0.311 nm/%RH (in the decreasing RH graph), with correlations of 0.9968 and 0.9934 respectively. Sensitivity significantly rises at higher RH, presenting superior values of 1.352 nm/%RH (increasing RH) and 1.324 nm/%RH (diminishing RH) and linear correlations of 0.9993 and 0.9995. These values of sensitivity and linearity improve on some of the very recently reported humidity optical fiber sensors [41, 42].

Particularly in our case, the substantial gain of sensitivity relies on the nature and extent of H-bonding within the sensitive thin film [43]. At lower hydration levels, water molecules are mainly adsorbed on the surface protonated groups of PEI and on the surface hydrophilic groups of GO [9]. Nonetheless, an increase in humidity promotes the diffusion of water molecules into the bulk of the thin film, being arbitrarily adsorbed in the hydrophilic functionalities of PEI and GO [9]. Furthermore, due to the super permeability of the GO to water molecules [44, 45], at high RH values water molecules can be continuously adsorbed, as the multilayer physical adsorption of water within the thin film occurs [46]. Hence, water molecules become mobile and gradually more equal to those in the bulk liquid [46]; consequently, the H-bond network is dominated by links between water units present within the layers of the sensitive coating [43, 46].

The average resolution of the fabricated sensor over the entire range of RH is 2.5 %RH. Nevertheless, the resolution significantly enhances at high RH, where the sensor is much more sensitive. In the RH interval from 70 % - 90 % it is possible to detect changes of 1.1 %RH.

3.4. Dynamic Response

To study the dynamic response of the sensor, it was introduced into the environmental chamber where the RH was set to continuously increase and switch from 20 % to 90 % at 20 °C at a rate of 0.8 %HR per minute. The RH has been simultaneously monitored by the capacitive humidity sensor fitted in the environmental chamber, as shown in Figure 7.

The fabricated sensor exhibits reproducible adsorption and desorption evolutions, demonstrating good repeatability and stability of the reference line (Figure 7). Additionally, the response of the optical fiber sensor is very sharp at high RH, which means this device is more sensitive at greater wetness values. This evolution confirms the previously discussed findings on the static response.

The dynamic performance of this device has been also tested as a breathing sensor. The response of the instrument was monitored and recorded while a person blew over the fabricated device. Figure 8 shows the wavelength shift for five human breathing cycles corresponding to the real time breathing response. The sensor tracks the rapid humidity rises and falls with alacrity and it recovers fully and returns to its initial baseline.

The developed sensor shows fast as well as stable response and recovery. The response and recovery times have been estimated as the required time to go from 10 % to 90 % of the maximum wavelength shift value and *vice versa*. Figure 9 displays a zoom-in of one of the breathing cycles to show in detail how reaction and retrieval times have been calculated.

This sensor is very rapid with a response time of 160 ms and recovery of 262 ms, which demonstrates the suitability of the sensing material for monitoring rapid humidity changes. In addition, it is much faster than other very recently reported optical fiber humidity sensors, such as 2.73 s reaction and 7.27 s recovery in [41], 1 s rinsing time and 5 s retrieval in [47] and 1.5 s and 4 s in [48]. To the best of the authors' knowledge, this optical fiber humidity sensor has one of the promptest recovery durations ever reported. Ultrafast optical sensors based on optical fibers could show a slightly faster response of about 50 ms [49] but a noticeably slower recovery (>700 ms to recover) [49].

4. CONCLUSIONS

In summary, a very rapid, stable and sensitive humidity LMR optical fiber sensor has been fabricated. Dip-assisted layer-by-layer assembly has been proven as a successful deposition technique to fabricate good quality films with controlled thickness, which is essential for this type of sensor. The hysteresis of this sensor is excellent. It shows a much greater sensitivity at high RH due to the diffusion of water molecules into the bulk of the thin film, where water molecules are adsorbed and form continuous multilayers.

The dynamic response of the developed device has been characterized in an environmental chamber and as a breathing sensor. It exhibits very fast reaction time and, especially, extremely rapid recovery periods, improving on those of some ultrafast optical fiber sensors

found in the literature. To the extent of the authors' knowledge, this is the first LMR optical fiber humidity sensor incorporating GO as part of the sensing coating.

'Declarations of interest: none'

ACKNOWLEDGEMENTS

Special thanks to the National EPSRC XPS User Service (NEXUS) at Newcastle for the support with the surface chemistry characterization. We also thank our colleagues from UPNA Sensors Research Group (Universidad Pública de Navarra, Spain) who lent us some of their facilities and provided support to operate them.

This research did not receive any specific grant from funding agencies in the public, commercial, or not-for-profit sectors.

REFERENCES

1. Zampolli, S., et al., *Selectivity enhancement of metal oxide gas sensors using a micromachined gas chromatographic column.* Sensors and Actuators B-Chemical, 2005. **105**(2): p. 400-406.
2. Ying, J.R., C.R. Wan, and P.J. He, *Sol-gel processed TiO2-K2O-LiZnVO4 ceramic thin films as innovative humidity sensors.* Sensors and Actuators B-Chemical, 2000. **62**(3): p. 165-170.
3. Jain, M.K., M.C. Bhatnagar, and G.L. Sharma, *Effect of Li+ doping on ZrO2-TiO2 humidity sensor.* Sensors and Actuators B-Chemical, 1999. **55**(2-3): p. 180-185.
4. Saha, D., et al., *Magnesium chromate-TiO2 spinel tape cast thick film as humidity sensor.* Sensors and Actuators B-Chemical, 2005. **107**(1): p. 323-331.
5. Sakai, Y., *Humidity Sensors Using Chemically-Modified Polymeric Materials.* Sensors and Actuators B-Chemical, 1993. **13**(1-3): p. 82-85.
6. Chachulski, B., et al., *Properties of a polyethyleneimine-based sensor for measuring medium and high relative humidity.* Measurement Science and Technology, 2006. **17**(1): p. 12-16.
7. Sakai, Y., Y. Sadaoka, and M. Matsuguchi, *Humidity sensors based on polymer thin films.* Sensors and Actuators B-Chemical, 1996. **35**(1-3): p. 85-90.
8. Harsanyi, G., *Polymeric Sensing Films - New Horizons in Sensorics.* Sensors and Actuators a-Physical, 1995. **46**(1-3): p. 85-88.
9. Tai, H.L., et al., *Facile development of high performance QCM humidity sensor based on protonated polyethylenimine-graphene oxide nanocomposite thin film.* Sensors and Actuators B-Chemical, 2016. **230**: p. 501-509.
10. Wang, X.F., et al., *Highly sensitive humidity sensors based on electro-spinning/netting a polyamide 6 nano-fiber/net modified by polyethyleneimine.* Journal of Materials Chemistry, 2011. **21**(40): p. 16231-16238.
11. Sakai, Y., Y. Sadaoka, and K. Ikeuchi, *Humidity Sensors Composed of Grafted Copolymers.* Sensors and Actuators, 1986. **9**(2): p. 125-131.
12. Sakai, Y., M. Matsuguchi, and T. Hurukawa, *Humidity sensor using cross-linked poly(chloromethyl styrene).* Sensors and Actuators B-Chemical, 2000. **66**(1-3): p. 135-138.

13. Su, P.G. and X.R. Kuo, *Low-humidity sensing properties of carboxylic acid functionalized carbon nanomaterials measured by a quartz crystal microbalance.* Sensors and Actuators a-Physical, 2014. **205**: p. 126-132.
14. Su, P.G. and Z.M. Lu, *Flexibility and electrical and humidity-sensing properties of diamine-functionalized graphene oxide films.* Sensors and Actuators B-Chemical, 2015. **211**: p. 157-163.
15. Lei, S., D.J. Chen, and Y.Q. Chen, *A surface acoustic wave humidity sensor with high sensitivity based on electrospun MWCNT/Nafion nanofiber films.* Nanotechnology, 2011. **22**(26).
16. Yao, Y., et al., *Graphene oxide thin film coated quartz crystal microbalance for humidity detection.* Applied Surface Science, 2011. **257**(17): p. 7778-7782.
17. Hernaez, M., et al., *Optical Fibre Sensors Using Graphene-Based Materials: A Review.* Sensors, 2017. **17**(1).
18. Toda, K., R. Furue, and S. Hayami, *Recent progress in applications of graphene oxide for gas sensing: A review.* Analytica Chimica Acta, 2015. **878**: p. 43-53.
19. Lee, C.Y. and G.B. Lee, *Humidity sensors: A review.* Sensor Letters, 2005. **3**(1): p. 1-15.
20. Culshaw, B., *Optical fiber sensor technologies: Opportunities and-perhaps-pitfalls.* Journal of Lightwave Technology, 2004. **22**(1): p. 39-50.
21. Culshaw, B. and A. Kersey, *Fiber-optic sensing: A historical perspective.* Journal of Lightwave Technology, 2008. **26**(9-12): p. 1064-1078.
22. Sharma, A.K., R. Jha, and B.D. Gupta, *Fiber-optic sensors based on surface plasmon resonance: A comprehensive review.* Ieee Sensors Journal, 2007. **7**(7-8): p. 1118-1129.
23. Del Villar, I., et al., *Optical sensors based on lossy-mode resonances.* Sensors and Actuators B-Chemical, 2017. **240**: p. 174-185.
24. Borges, J. and J.F. Mano, *Molecular Interactions Driving the Layer-by-Layer Assembly of Multilayers.* Chemical Reviews, 2014. **114**(18): p. 8883-8942.
25. Li, Y., X. Wang, and J.Q. Sun, *Layer-by-layer assembly for rapid fabrication of thick polymeric films.* Chemical Society Reviews, 2012. **41**(18): p. 5998-6009.
26. Xu, G.R., et al., *Layer-by-layer (LBL) assembly technology as promising strategy for tailoring pressure-driven desalination membranes.* Journal of Membrane Science, 2015. **493**: p. 428-443.
27. Iler, R.K., *Multilayers of Colloidal Particles.* Journal of Colloid and Interface Science, 1966. **21**(6): p. 569-+.
28. Sui, Z.Y., et al., *Preparation of Three-Dimensional Graphene Oxide-Polyethylenimine Porous Materials as Dye and Gas Adsorbents.* Acs Applied Materials & Interfaces, 2013. **5**(18): p. 9172-9179.
29. Sanchez, P., et al., *Optical fiber refractometers based on Lossy Mode Resonances by means of SnO2 sputtered coatings.* Sensors and Actuators B-Chemical, 2014. **202**: p. 154-159.
30. Hernaez, M., A.G. Mayes, and S. Melendi-Espina, *Graphene Oxide in Lossy Mode Resonance-Based Optical Fiber Sensors for Ethanol Detection.* Sensors, 2018. **18**(1).
31. Hernaez, M., Mayes, A.G., Melendi-Espina, S., *Sensitivity enhancement of lossy mode resonance-based ethanol sensors by graphene oxide coatings*, in *IEEE Sensors 2017 Proceedings*. 2017: Glasgow, UK. p. Paper 1450.
32. Zhao, L.L., et al., *Preparation of graphene oxide/polyethyleneimine layer-by-layer assembled film for enhanced hydrogen barrier property.* Composites Part B-Engineering, 2016. **92**: p. 252-258.
33. Aleksandrzak, M., et al., *Effect of graphene thickness on photocatalytic activity of TiO2-graphene nanocomposites.* Applied Surface Science, 2015. **331**: p. 193-199.
34. Hontorialucas, C., et al., *Study of Oxygen-Containing Groups in a Series of Graphite Oxides - Physical and Chemical Characterization.* Carbon, 1995. **33**(11): p. 1585-1592.

35. Wang, G.X., et al., *Synthesis of enhanced hydrophilic and hydrophobic graphene oxide nanosheets by a solvothermal method.* Carbon, 2009. **47**(1): p. 68-72.
36. He, L., et al., *Poly(ethyleneimine) functionalized organic-inorganic hybrid silica by hydrothermalassisted surface grafting method for removal of nickel(II).* Korean Journal of Chemical Engineering, 2014. **31**(2): p. 343-349.
37. Poh, H.L., et al., *Graphenes prepared by Staudenmaier, Hofmann and Hummers methods with consequent thermal exfoliation exhibit very different electrochemical properties.* Nanoscale, 2012. **4**(11): p. 3515-3522.
38. Pei, S.F. and H.M. Cheng, *The reduction of graphene oxide.* Carbon, 2012. **50**(9): p. 3210-3228.
39. Arregui, F.J., et al., *Giant sensitivity of optical fiber sensors by means of lossy mode resonance.* Sensors and Actuators B-Chemical, 2016. **232**: p. 660-665.
40. Zamarreno, C.R., et al., *Optical Fiber Humidity Sensor Based on Lossy Mode Resonances Supported by TiO2/PSS Coatings.* Eurosensors Xxv, 2011. **25**.
41. Huang, Y.M., et al., *High-performance fibre-optic humidity sensor based on a side-polished fibre wavelength selectively coupled with graphene oxide film.* Sensors and Actuators B-Chemical, 2018. **255**: p. 57-69.
42. Sanchez, P., et al., *Lossy mode resonances toward the fabrication of optical fiber humidity sensors.* Measurement Science and Technology, 2012. **23**(1).
43. Medhekar, N.V., et al., *Hydrogen Bond Networks in Graphene Oxide Composite Paper: Structure and Mechanical Properties.* Acs Nano, 2010. **4**(4): p. 2300-2306.
44. Wei, N., X.S. Peng, and Z.P. Xu, *Understanding Water Permeation in Graphene Oxide Membranes.* Acs Applied Materials & Interfaces, 2014. **6**(8): p. 5877-5883.
45. Boukhvalov, D.W., M.I. Katsnelson, and Y.W. Son, *Origin of Anomalous Water Permeation through Graphene Oxide Membrane.* Nano Letters, 2013. **13**(8): p. 3930-3935.
46. Bi, H.C., et al., *Ultrahigh humidity sensitivity of graphene oxide.* Scientific Reports, 2013. **3**.
47. Luo, Y.H., et al., *Tungsten disulfide (WS2) based all-fiber-optic humidity sensor.* Optics Express, 2016. **24**(8): p. 8956-8966.
48. Ascorbe, J., et al., *High sensitivity humidity sensor based on cladding-etched optical fiber and lossy mode resonances.* Sensors and Actuators B-Chemical, 2016. **233**: p. 7-16.
49. Mathew, J., Y. Semenova, and G. Farrell, *A fiber bend based humidity sensor with a wide linear range and fast measurement speed.* Sensors and Actuators a-Physical, 2012. **174**: p. 47-51.

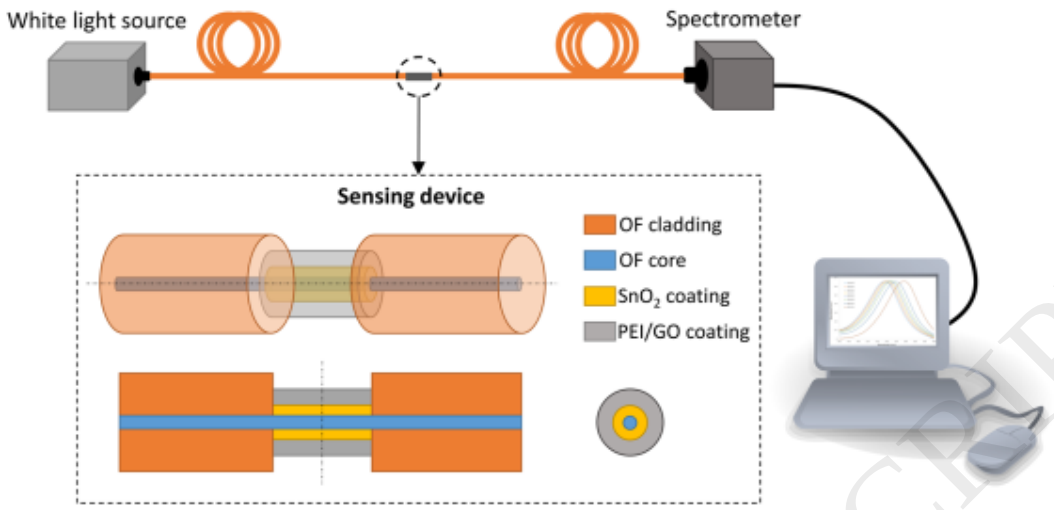

Figure 1. Optical fiber experimental setup and sensor schematic structure with longitudinal and cross-sections.

Figure 1. Optical fiber experimental setup and sensor schematic structure with longitudinal and cross-sections.

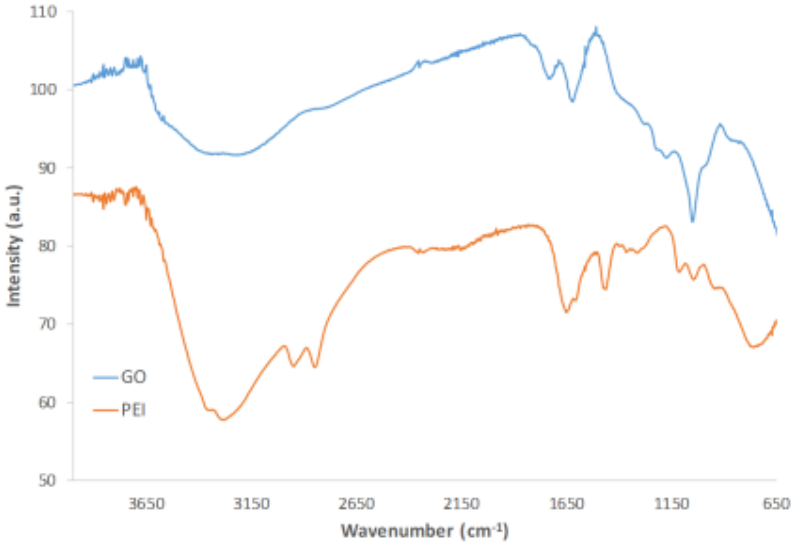

Figure 2. FT-IR spectra of GO and PEI.

Figure 2. FT-IR spectra of GO and PEI.

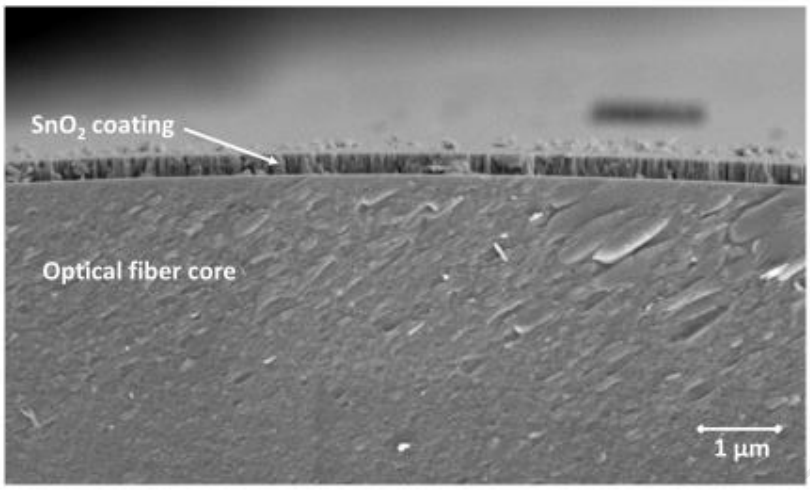

Figure 3. SEM image of the SnO_2-coated optical fiber core.

Figure 3. SEM image of the SnO_2-coated optical fiber core.

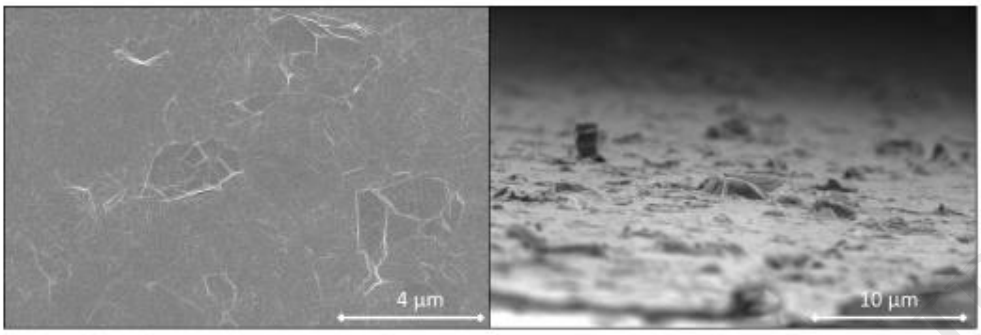

Figure 4. Images of the superficial structure of a 5-bilayer PEI/GO coating deposited onto glass slide.

Figure 4. Images of the superficial structure of a 5-bilayer PEI/GO coating deposited onto glass slide.

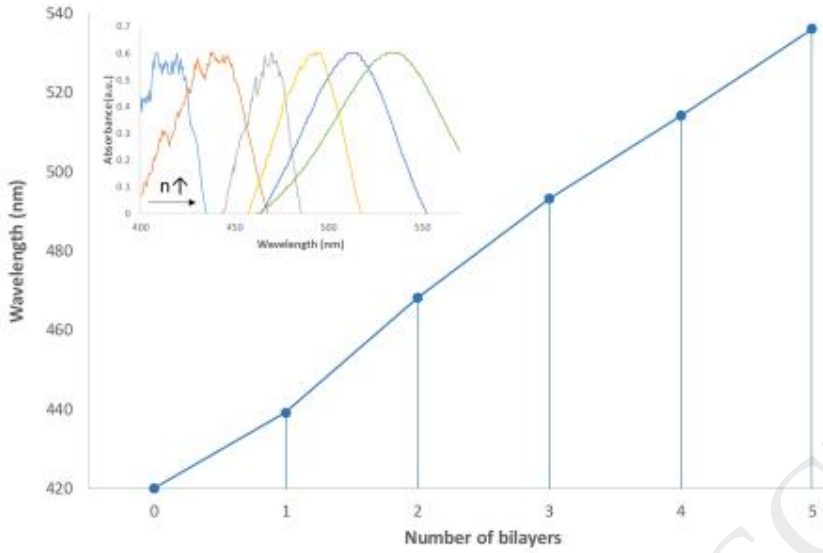

Figure 5. Shift of the LMR absorption peak generated by the SnO_2 coated fiber during the deposition of five bilayers of PEI/GO.

Figure 5. Shift of the LMR absorption peak generated by the SnO_2 coated fiber during the deposition of five bilayers of PEI/GO.

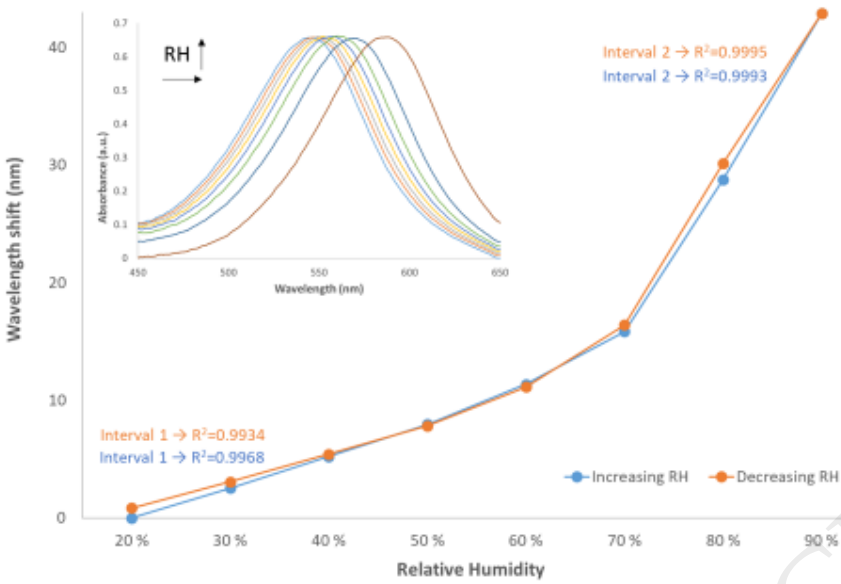

Figure 6. Shift of the LMR absorption peak generated by the sensor when it is introduced in an environmental chamber and the RH is varied from 20 %-90 % (blue line) and from 90 % to 20 % (orange line).

Figure 6. Shift of the LMR absorption peak generated by the sensor when it is introduced in an environmental chamber and the RH is varied from 20 %-90 % (blue line) and from 90 % to 20 % (orange line).

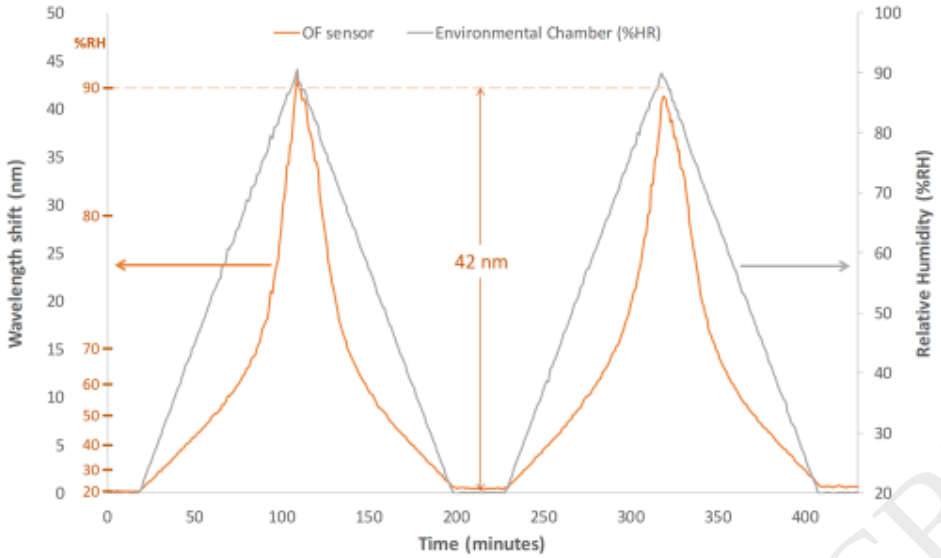

Figure 7. Dynamic response in an environmental chamber.

Figure 7. Dynamic response in an environmental chamber.

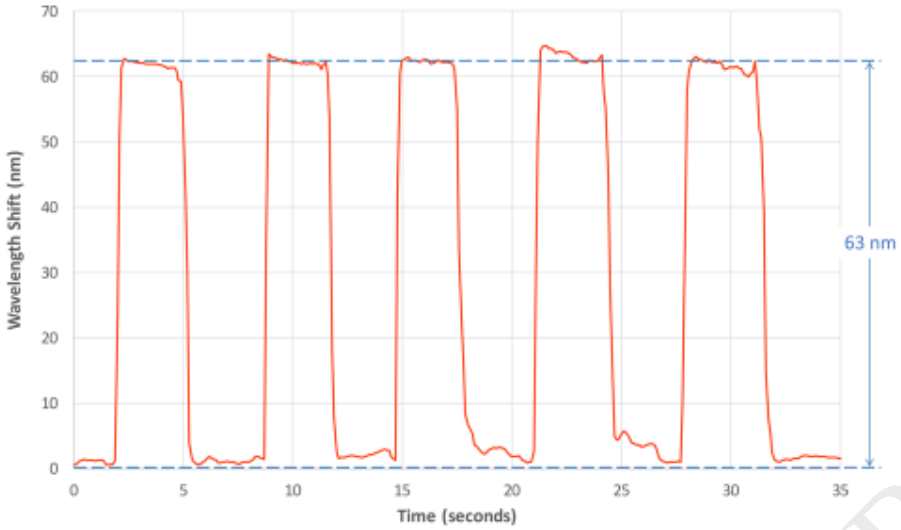

Figure 8. Dynamic response of the developed sensor corresponding to five human breathing cycles.

Figure 8. Dynamic response of the developed sensor corresponding to five human breathing cycles.

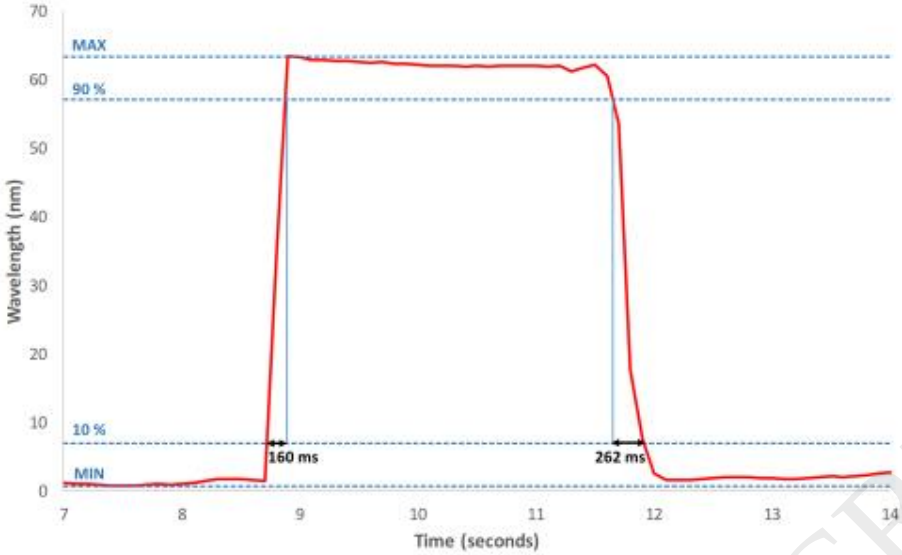

Figure 9. Zoom-in of one of the breathing cycles.

Figure 9. Zoom-in of one of the breathing cycles.

Table 1. Surface composition of the selected GO and functional groups by curve fitting of C(1s) spectrum.

	C (at%)	O (at%)	C/O	Csp^2 (%)	Csp^3 (%)	C-OH/C-O-C (%)	C=O (%)	COOH (%)	π*-π* (%)
GO	68.2	31.8	2.1	16.2	28.4	36.9	10.8	7.0	0.7